Heart and Vessels (2019) 34:74–83
https://doi.org/10.1007/s00380-018-1209-2

ORIGINAL ARTICLE

Evaluation of the pulmonary artery potential using a 20-polar circumferential catheter and three-dimensional integrated intracardiac echocardiography

Masayuki Takahashi[1] · Hisashi Yokoshiki[2] · Hirofumi Mitsuyama[3] · Taro Tenma[1] · Masaya Watanabe[1] · Rui Kamada[1] · Ryo Sasaki[4] · Yuki Chiba[4] · Motoki Maeno[4] · Toshihisa Anzai[1]

Received: 27 March 2018 / Accepted: 15 June 2018 / Published online: 21 June 2018

Abstract
Prolongation of the pulmonary artery potentials (PAPs) in response to short coupling intervals was related to polymorphic QRS configurations during the ventricular tachycardia originating above the pulmonary valve (PA-VT). This prospective study was aimed to investigate the mechanisms of polymorphic changes during the PA-VT. We performed the mapping above the pulmonary valve using a 20-polar circumferential catheter and three-dimensional integrated intracardiac echocardiography in 9 consecutive patients with outflow tract arrhythmias undergoing catheter ablation (UMIN ID: UMIN000021682). The location of successful ablation was right ventricular outflow tract (RVOT) in 6 patients, above the pulmonary valve in 1 patient, left coronary cusp in 1 patient, and unknown in 1 patient. The PAP was detected in six (67%) patients with bipolar voltage of 0.56 ± 0.27 mV. Pacing from bipolar electrodes of the circumferential catheter located above the pulmonary valve captured the PA myocardium only in 1 patient who had the PA-VT (100% in PA-VT vs 0% in non-PA-VT, $P = 0.0046$), and slight changes of the QRS morphology was observed in accordance with the conduction delay from the stimulus to activation of the RVOT myocardium. The selective PAP capture with conduction delays evoked by bipolar stimulations through a 20-polar circumferential catheter may be a characteristic property of patients with the PA-VT. Conduction delays within the PA and PA-RVOT junction appears to contribute polymorphic QRS changes during the PA-VT.

Keywords Ventricular tachycardia · Polymorphic · Pulmonary artery potential · Pulmonary valve · Intracardiac echocardiography

Introduction

Prevalence of idiopathic ventricular arrhythmias (VAs) originating above the pulmonary valve (PA-VAs) ranged from 6 to 90% among the right ventricular outflow tract (RVOT) arrhythmias [1–8]. These disparities would depend on the difference in study populations, as well as methods used for determining the location of origins of these arrhythmias, most of which were pulmonary arteriography and/or right ventriculography. At present, only one study used three-dimensional integrated intracardiac echocardiography to localize the pulmonary valve, and found that 46% of RVOT arrhythmia foci were above the pulmonary valve with a median distance of 8.2 mm [2]. Thus, the PA-VAs are likely to be more common than previously thought, although there are still ongoing debates with regard to the true incidence of PA-VAs and the ablation method for RVOT/PA arrhythmias [9–11].

Despite idiopathic, there is a malignant form of ventricular tachycardia arising above the pulmonary valve (PA-VT), because it activates rapidly [6, 12], sometimes shows a polymorphic QRS configuration [6, 13–15], and triggers ventricular fibrillation with a rare occasion [6, 14]. We also

✉ Hisashi Yokoshiki
hisashi.yokoshiki@doc.city.sapporo.jp

[1] Department of Cardiovascular Medicine, Hokkaido University Graduate School of Medicine, Sapporo, Japan

[2] Department of Cardiovascular Medicine, Sapporo City General Hospital, Kita-11, Nishi-13, Chuo-ku, Sapporo 060-8604, Japan

[3] Department of Cardiovascular Medicine, Hokkaido Ohno Memorial Hospital, Sapporo, Japan

[4] Division of Medical Engineering Center, Hokkaido University Hospital, Sapporo, Japan

observed, during the PA-VT, the QRS morphology altered in association with increase in the pulmonary artery potential (PAP) duration [6]. Liu et al. reported that, among 12 patients with the PA-VAs, three VTs (2 sustained and 1 non-sustained) were induced in the presence of isoproterenol and terminated by administration of adenosine, suggesting the cAMP-mediated triggered activity from focal origins [2, 16]. However, the mechanism of its polymorphic alteration remains to be elucidated.

We hypothesized that the rapid focal activation above the pulmonary valve produces the heterogeneous conduction which propagates through the ventriculo-arterial junction alternating the exit sites, thereby showing polymorphic VT. The present study is aimed to test this hypothesis using a 20-polar circumferential catheter for recording and pacing the PAP and intracardiac echocardiography (ICE) for delineating the sites of attachment of the pulmonary valves.

Methods

Subjects

We prospectively enrolled 9 patients in the Hokkaido Outflow Tract Ventricular Tachycardia Study (HOT-VT) (UMIN ID: UMIN000021682) which was approved by the Ethics Committee of Hokkaido University Hospital. Patients undergoing catheter ablation for VAs of a left bundle branch block (LBBB)-like QRS morphology and inferior axis were eligible in this study. The study period was from April 2016 to November 2017.

Table 1 Patient characteristics

	Total ($n=9$)
Age (years)	44 ± 5
Male	7 (78%)
LVEF (%)	56 ± 4
Syncope	2 (22%)
PVC-induced cardiomyopathy	2 (22%)
ICD, *n* (%)	1 (11%)
VT/PVC	4 (44%)/5 (56%)
Polymorphic VT	1 (11%)
Presence of PAP	6 (67%)
Arrhythmia origin	
Pulmonary artery	1 (11%)
RVOT	6 (67%)
Left coronary cusp	1 (11%)
Unknown	1 (11%)

Data are given as mean ± SE or *n* (%)

LVEF left ventricular ejection fraction, *PVC* premature ventricular contraction, *ICD* implantable cardioverter-defibrillator, *VT* ventricular tachycardia, *PAP* pulmonary artery potential, *RVOT* right ventricular outflow tract

Electrophysiological study

After obtaining written informed consent, the electrophysiological study was performed with no antiarrhythmic agents in the fasting state. Using a 10 F phased-array ICE catheter (SoundStar; Biosense Webster Inc, Diamond Bar, CA, USA) with the CARTO 3 system (Biosense Webster Inc), the anatomic map of the RVOT and PA was created. Special attention was paid to delineate the pulmonic valve annulus which was determined by the attachment position of pulmonary valve leaflets. Based on this anatomic map and fluoroscopic images, a 20-pole circumferential catheter (Lasso, 25–15 mm; Biosense Webster, Inc.) was placed immediately above the pulmonary valve through a steerable introducer (Agilis; St Jude Medical, St. Paul, MN, USA). A 4 mm-tip quadripolar ablation catheter (NaviStar; Biosense Webster Inc.) and a quadripolar catheter were positioned at the septal side of RVOT and right ventricular apex (RVA), respectively.

Pacing protocol

Burst pacing and extrastimulus S1 (baseline pacing) S2S3 (premature stimulation) pacing protocols were applied through bipolar electrodes of a 20-polar circumferential catheters (located above the pulmonary valve) and distal pairs of bipolar electrodes of a quadripolar catheter

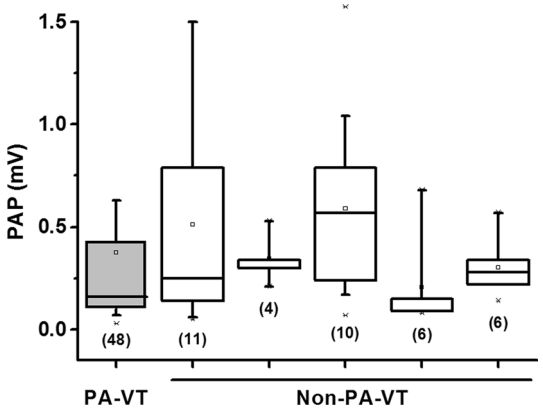

Fig. 1 Summary of the amplitude of pulmonary artery potential (PAP) in patients with the PA-VT and non-PA-VT. This graph shows the box-and-whisker plots of the PAP amplitude in each patient. The vertical line and open square indicates the median and average amplitude, respectively. The size of the box represents interquartile range (IQR). Number of PAPs, recorded from a 20-polar circumferential catheter and an ablation catheter, are given in parentheses. As the voltage mapping above the PA valve using an ablation catheter was not performed prospectively, the number of mapping points differs among these patients

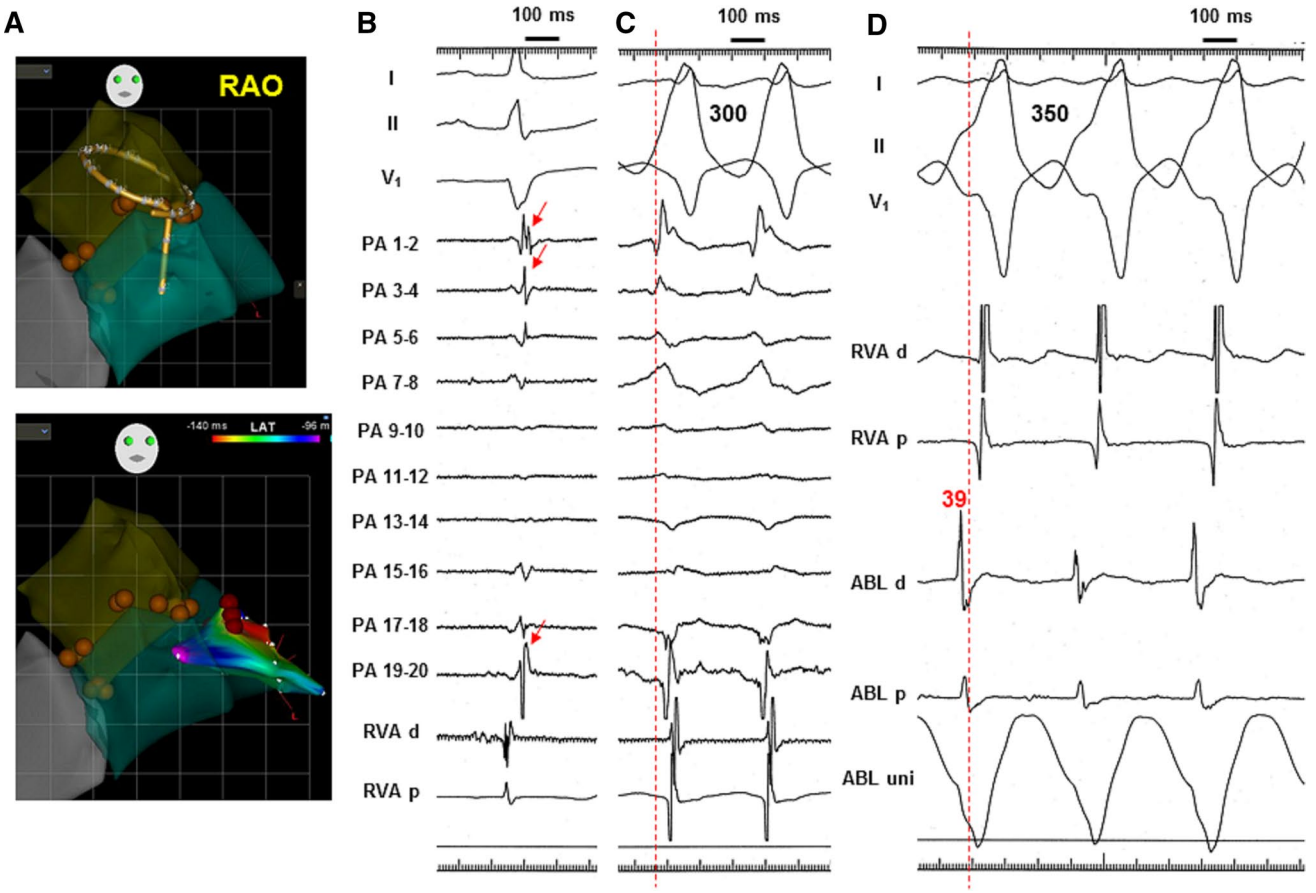

Fig. 2 The pulmonary artery potential (PAP) in a patient with the RVOT-VT. **a** Anatomical images constructed using an ICE catheter with the CARTO 3 system. An upper panel shows a 20-polar circumferential catheter placed in the PA. Brown tags indicate location of the ICE-defined pulmonic valve annulus. A lower panel shows the superimposed anatomical image and ablation sites (dark red tags). The PA and RVOT (below the PA valve) are separated by the PA valve, and are colorized in brown and blue, respectively. RAO: right anterior oblique. **b** Surface ECGs (leads I, II, and V1) and intracardiac electrograms recorded from the PA and right ventricular apex (RVA d and RVA p, distal and proximal pairs of electrodes of a quadri-polar catheter) during sinus rhythm. PA 1–2 to 19–20 were bipolar recordings with a 20-polar circumferential catheter in the PA. Red arrows indicate the PAP which activates during the late phase of the QRS complex [4, 12]. **c** During the rapid non-sustained VT episode, the PAP did not precede the QRS wave, but was fused with a far field myocardial potential of the RVOT. A red dotted vertical line denotes the onset of QRS wave. **d** During the sustained VT with a cycle length of 350 ms, a 4-mm tip ablation catheter (NaviStar; Biosense-Webster, Inc) was placed at the RVOT just below the PA valve (red tags in the lower panel of Fig. 2a). Ventricular electrogram recorded from the ablation catheter preceded the QRS wave by 39 ms. ABL d and ABL p: distal and proximal pairs of electrodes of an ablation catheter; ABL uni: unipolar recording from a distal electrode of an ablation catheter

(located at the RVOT and RVA). At the three pacing sites, changes in QRS morphology were evaluated by quantitative morphology-matching software (PaSo; Biosense Webster Inc) based on a QRS morphology at the pacing cycle length of 400 ms as a reference. Pacing output was set about twofold of the threshold and the maximum value was 9.9 V with a pulse width of 1 ms. During the burst pacing protocol, eight stimulations were delivered with an initial pacing cycle length of 400 ms. Then, the pacing cycle length was shortened with 10 ms decrement until loss of 1:1 capture or 200 ms. For the extrastimulus pacing protocol, effective refractory period (ERP) was initially measured at the basic cycle length of 400 ms. After eight baseline (S1) beats at the pacing cycle length of 400 ms, the S1S2 interval was set (a) 280 ms or (b) ERP plus 20 ms, and the S2S3 interval was shortened successively in steps of 10 ms until loss of capture. A QRS morphology-match score at the shortest S2S3 interval was obtained at each pacing site.

Ablation procedure

Target VAs were induced spontaneously in 5 patients, by programmed ventricular stimulation in 1 patient, and by intravenous administration of isoproterenol at a dose of

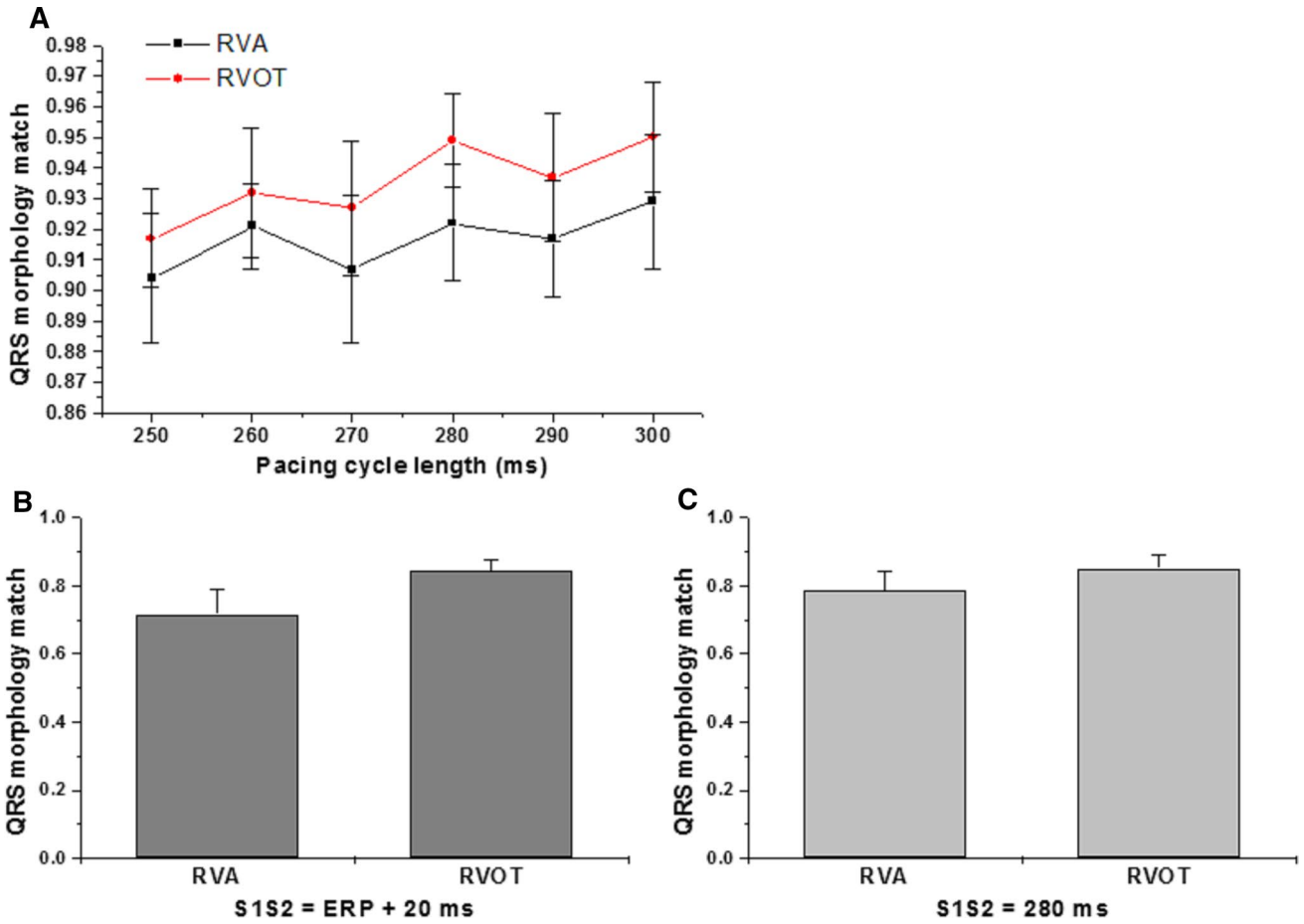

Fig. 3 QRS Morphology Match using the PaSo Software during the Pacing Study. Burst (**a**) and (**b**, **c**) extrastimulus pacing from right ventricular apex (RVA) and right ventricular outflow tract (RVOT). See text in details

1–4 µg/min in 2 patients. The VA of one patient was non-inducible by any protocol, and ablation was performed based on the QRS morphology of the VA recorded before the procedure. A 4-mm tip ablation catheter (NaviStar; Biosense-Webster, Inc) was inserted into the right ventricle (RV) via a right femoral vein. The earliest activation site of the VAs was usually targeted. Radiofrequency (RF) energy was applied at a maximum of 35 W provided that temperature recorded from the electrode did not reach more than 55 °C. Energy application at one site was usually terminated for 60 s. A successful ablation site was confirmed by the anatomic map which had been created using an ICE catheter and the CARTO 3 system (see above).

Statistical analysis

All data are expressed as means ± SE. Simple between-group analyses were conducted using a Student's *t* test. Categorical variables were compared using Chi-square test. Differences with $P < 0.05$ were considered significant.

Results

Patient characteristics

The characteristics of 9 patients are shown in Table 1. An arrhythmic origin determined by a successful ablation site was pulmonary artery (PA) in 1 patient, RVOT in 6 patients, left coronary cusp in 1 patient. An exact origin was unknown in 1 patient, because any target VAs did not occur during the ablation procedure. A history of syncope was noted in two patients, whose arrhythmic origin was PA and RVOT, respectively. Due to recurrent VAs with syncope, a patient with the PA-VT had received an implantable cardioverter-defibrillator (ICD) in his previous hospital.

Recording and pacing above the PA valve using a 20-polar circumferential catheter

A 20-polar circumferential catheter was placed above the PA valve with a minimum distance of 4.2 ± 0.8 mm from the valve leaflet attachment. PAP was recorded in 6 patients

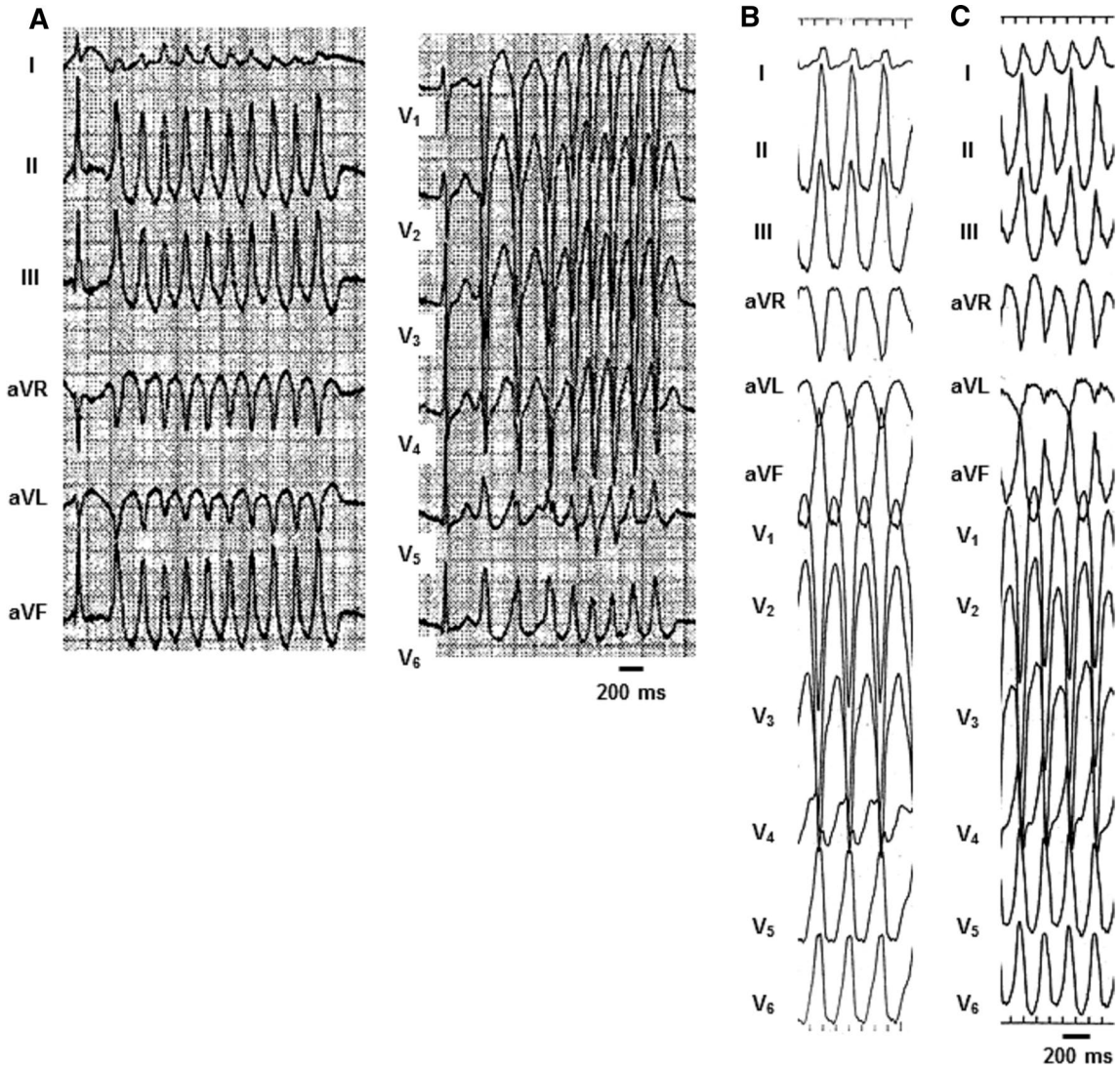

Fig. 4 Twelve-Lead ECGs during ventricular tachycardias (VTs) originating above the pulmonary artery (PA) valve. **a** A non-sustained VT with polymorphic QRS changes especially in precordial leads. The ECGs in limb leads and precordial leads were recorded separately, that is two episodes of the VT. **b** A monomorphic VT with a cycle length of 280 ms. **c** A VT with beat-by-beat alternating QRS complexes

(67%). The maximal amplitude of the PAPs recorded from the bipolar electrodes was 0.56 ± 0.27 mV in 6 patients (mean $\pm$ SE, $n = 6$). Location of the maximal PAP was above the left (posterior) semilunar valve in 3 patients, above the anterior semilunar valve in 2 patients, and above the right semilunar valve in 1 patient. The PA myocardium extended with the average length of 25.0 ± 3.0 mm along the circumferential catheter ($n = 6$). In a patient with the PA-VT, the maximal PAP of 0.39 mV was observed above the right semilunar valve and its extension length along the catheter was 22 mm.

We also evaluated the amplitude of all the PAP recorded from not only a 20-polar circumferential catheter but also an ablation catheter in each patient (Fig. 1). The median and average amplitude was 0.16 mV and 0.37 mV in the PA-VT patient, which were not distinguishable from those in the non-PA-VT patients.

Figure 2 shows an example of the PAP in a patient with the RVOT-VT. A sharp potential during the late phase of the QRS complex is considered to be the activation of myocardial extensions in the PA, that is PAP (Fig. 2b), as previously reported [4, 12]. Pacing through bipolar electrodes of the catheter captured the PA only in 1 patient with the PA-VT, whereas the PA capture was not observed even with the maximal output in 7 patients, who had the VAs of non-PA origins (PA capture: 100% in the PA-VT vs 0% in the non-PA VAs, $P = 0.0046$). The shortest pacing cycle length of 1:1 PA capture was 360 ms in the patient with the PA-VT.

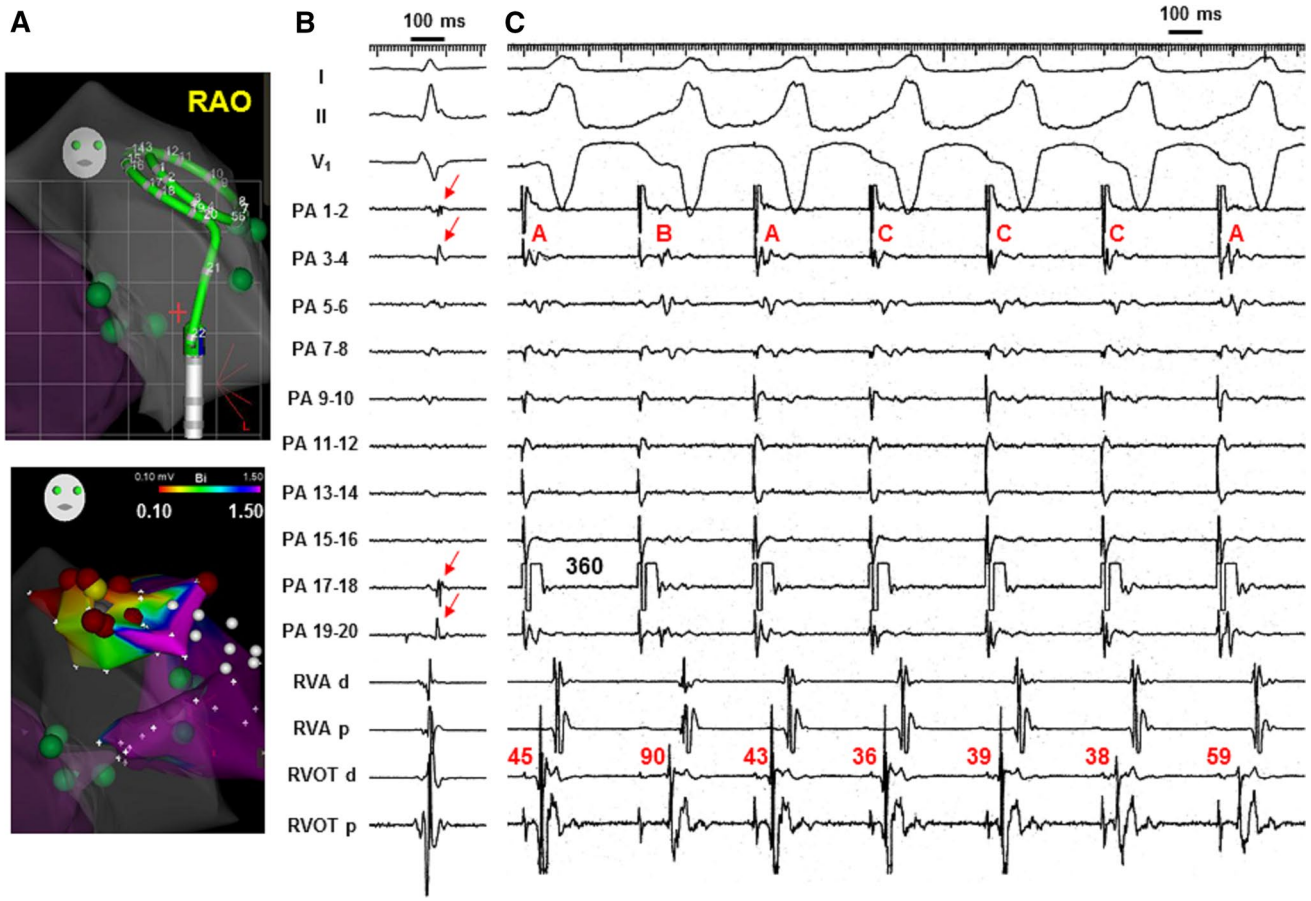

Fig. 5 Recording and pacing from the pulmonary artery (PA) in a patient with the PA-VT. **a** Anatomical images constructed using an ICE catheter with the CARTO 3 system. An upper panel shows a 20-polar circumferential catheter placed in the PA. Green tags indicate location of the ICE-defined pulmonic valve annulus. A lower panel shows the superimposed voltage map, ablation sites (dark red tags) and pulmonic valve annulus (green tags). RAO: right anterior oblique. **b** and **c** Surface ECGs (leads I, II, and V1) and intracardiac electrograms recorded from the PA, right ventricular apex (RVA d and RVA p, distal and proximal pairs of electrodes of a quadri-polar catheter) and right ventricular outflow tract (RVOT d and RVOT p, distal and proximal pairs of electrodes of a quadri-polar catheter) during sinus rhythm (**b**) and pacing from the PA (**c**). PA 1–2 to 19–20 were bipolar recordings with a 20-polar circumferential catheter in the PA. **b** Red arrows indicate the PAP. **c** Pacing was performed at a cycle length of 360 ms from bipolar electrodes of PA 17–18. Three patterns of the pacing delay were noted and were labelled with red-colored A, B and C above the tracing of PA 3–4. The numbers of red color indicate time intervals (ms) between the pacing stimulus to activation of RVOT (recorded from RVOT d)

For these reasons, the pacing study to compare changes in QRS morphology was not possible above the PA valve.

Pacing study

Burst pacing and extrastimulus pacing protocol at both RVA and RVOT were completed in 7 patients and 5 patients, respectively. QRS morphology match score during the burst pacing was comparable at the two sites (Fig. 3a). Loss of 1:1 capture occurred at the RVOT and/or RVA with the pacing cycle length less than 250 ms in some patients, and the paired analysis was appropriate at the pacing cycle length between 400 ms and 250 ms ($n=7$). The paired data regarding the extrastimulus pacing protocol were available in 5 patients. QRS morphology match score at the shortest S2S3 interval tended to be lower at the RVA than RVOT ($n=5$, $P=0.08$) with S1S2 interval of ERP plus 20 ms (Fig. 3b), but it was similar between the two sites with S1S2 interval of 280 ms (Fig. 3c). ERP was 212 ± 5 ms at the RVA and 228 ± 5 ms at the RVOT ($n=5$, $P<0.05$).

Case presentation: a patient with the PA-VT

A 56-year-old male was referred to our hospital for catheter ablation due to multiple appropriate ICD shocks. He had a history of recurrent syncope and polymorphic VT (Fig. 4a). At the electrophysiological laboratory, a monomorphic VT with a LBBB-type QRS morphology and inferior axis (Fig. 4b) and a VT with the QRS alternans (Fig. 4c) were induced. PAP was recorded through the 20-polar

circumferential catheters placed above the PA valve (Fig. 5a top panel, red arrows in Fig. 5b). Bipolar pacing at the cycle length of 360 ms through the PA 17–18 captured the PA with three different conduction patterns, which were noted by (a) the delay of PAP recorded at the PA 3–4 (patterns A, B and C in Fig. 5c) and (b) different time intervals from the pacing stimulus to electrogram recorded by distal poles of the RVOT (RVOT d) catheter (red number in Fig. 5c). Two patterns of conduction within the PA were also observed at the pacing cycle length of 370 ms (not shown). As the distance between the PA 17–18 and distal electrode of RVOT d was 17.6 mm, the conduction velocity (CV) could be calculated. With regard to the conduction between the PA and RVOT, the CV restitution curve can be drawn with three patterns (Fig. 6). Especially, the steep CV restitution with slow conduction (a black line in Fig. 6) was far more different, as compared with the CV between the RVOT and RVA that was constantly 1.1 m/s at the pacing cycle lengths of 400–360 ms (a flat CV restitution with normal conduction; the CV of 1.1 m/s was calculated based on the time interval of 45 ms from RVOT d to RVA d and the distance between distal electrodes of the two catheters, which was more than 50 mm.). Target VTs were induced by intravenous administration of isoproterenol. During the VT, the earliest activation was observed at the PA 19–20 and this PAP preceded the RVOT electrogram with variable time intervals (red number in Fig. 7). Application of RF energy (30 W, 55 °C) targeting the PAP (dark red tags in the lower panel of Fig. 5a) abolished the VT and the patient has been free from recurrence for more than 18 months.

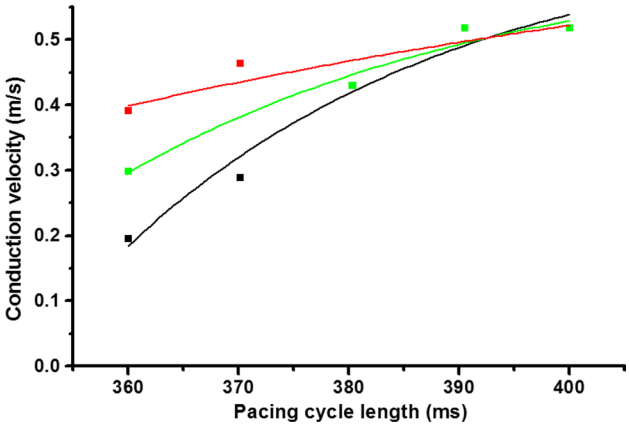

Fig. 6 Conduction velocity (CV) restitution curves of the PA myocardium. Note three curves can be illustrated based on different CVs in response to the same pacing cycle length, as shown in Fig. 3c. In addition, the CV less than 0.5 m/s was much slower than that (more than 1 m/s) in normal ventricular myocardium. Distance between the PA 17 electrode and distal electrode of the RVOT catheter was 17.6 mm

Discussion

This prospective study has demonstrated, with 3-D anatomical confirmation of the PA valve using an ICE, the PAP is present in 67% (6 out of 9) of patients who have VAs with a LBBB-type QRS morphology and inferior-axis. Among these patients, the selective PA capture was observed only in a patient with the PA-VT during bipolar pacing from a 20-polar circumferential catheter located in the PA (with a maximum output of 9.9 V/1 ms). Additionally, we recorded for the first time the activation patterns of PA myocardium during the PA-VT and found the mechanism of alterations in the QRS morphology was associated with the conduction delays in the PA and its junction to RVOT.

Hasdemir observed ventricular myocardial extensions beyond the attachment of pulmonary valve leaflets in 17% of ninety-five human hearts obtained at autopsy [17]. The extensions were noted above the pulmonary valve with the rate of 74% in a later study examining more than 600 autopsy hearts [18]. In addition, Yamasaki et al. reported the PA-VA slowly conducting over a suspected broad ventricular myocardial extension that exhibited beat-by-beat slight alternating QRS complexes and a relatively long stimulus-QRS interval of 59 ms during pace mapping in the PA [19]. Despite the limited number of patients in this study, the incidence of PAP recordings using a 20-polar circumferential catheter was 67%, which is in agreement with the recent study [18]. Interestingly, pacing from the circumferential catheter placed above the pulmonary valve captured the extended myocardium only in a patient with PA-VT. Whether or not the PAP of PA-VT has some specific property as initiator of malignant VAs requires further investigations.

A question arises why a pacing study could not be performed in the non-PA-VT patients if there was no difference with regard to the amplitude of the PA potentials between the PA-VT patient and non-PA-VT patients. We speculate that the heterogeneity of the voltages of PAPs (Fig. 1) and the possible difference in the width of propagation path between the PA and RVOT myocardium, i.e., an impedance mismatch between the sink and the source [20, 21], could determine whether there will be conduction or block. In addition, the pacing threshold can be greatly affected by the changes of the electrophysiological properties in myocardial sleeves [22], and such changes might be present between the arrhythmogenic and non-arrhythmogenic PA myocardium.

With regard to the changes of QRS morphology in response to burst and extrastimulus pacing, there was no significant difference between the two pacing sites of RVOT and RVA (Fig. 2). On the other hand, a patient with PA-VT exhibited the delayed and different patterns of conduction in the PA even at a pacing cycle length of 360 ms, thereby resulting in the steepness of CV restitution (Figs. 4 and

5). This is in contrast to RV myocardium which has a flat CV restitution at the pacing cycle lengths between 300 and 400 ms [23]. The slow and decremental conduction property in the PA was similar to that of a patient with polymorphic PA-VT in our previous study [6]. Steep CV restitution can be a major mechanism of spatial discordant alternans [24–28], as observed in our patient (Fig. 3c), and these observations would reinforce our hypothesis that ventricular extensions above the PA valve serve as the substrate for polymorphic VT [6].

Zhang et al. [8] have recently reported that, using an irrigation catheter with a reversed *U* curve, ablation at the PA cusp eliminated VAs of RVOT-type origin in 90% of the patients. In our six patients with RVOT-VT, the successful ablation site was confirmed using the CARTO Sound system at a mean distance of 5.1 ± 2.6 mm ($n = 6$) from the attachment of PA valve leaflet. Firm contact force at the PA cusp with an irrigation catheter could ablate the RVOT apex rather than by eliminating an arrhythmogenic origin within the cusp, because RF ablation with an irrigated electrode can create large lesion with a depth of more than 5 mm [29]. However, potential damage of left coronary artery should be taken into consideration due to the close proximity (< 5 mm) of the RVOT and pulmonary valve sinuses [10, 30]. Additionally, formation of a reversed *U* curve in the PA without damage to the pulmonary valves/sinuses may require advanced skills for catheter manipulation [10, 31]. In our five patients with malignant PA-VTs ([6] and a present case), successful elimination of these VAs was achieved using the conventional method. In contrast, Yagishita et al. [15] reported a case with polymorphic VTs originating from the PA, which was successfully abolished with an elegant

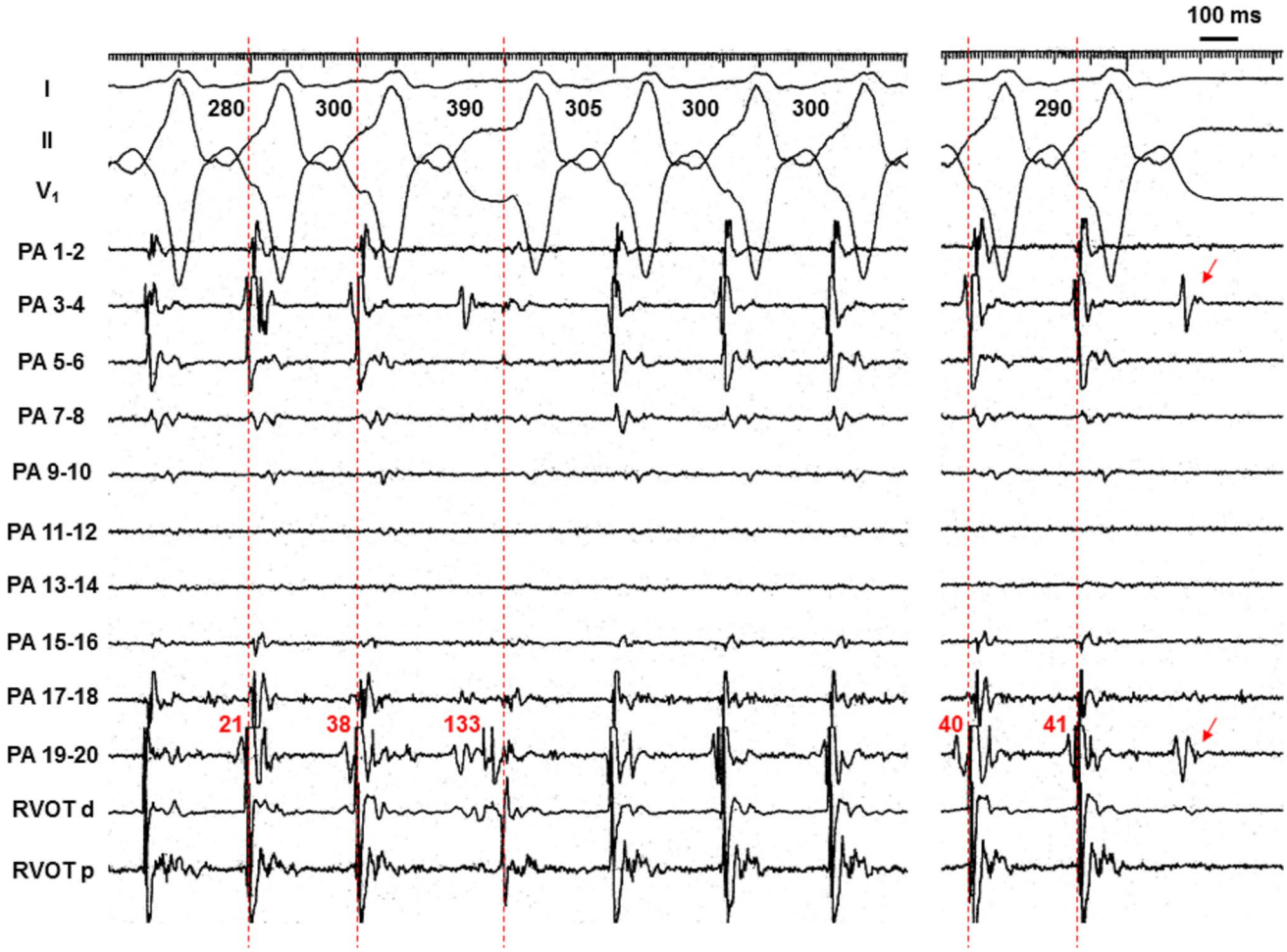

Fig. 7 Recordings of the PAP during the PA-VT. Shown are the surface ECGs, leads I, II, and V1, and intracardiac electrograms recorded from the PA and RVOT during the PA-VT. Note that slight morphological changes of QRS complexes and prolongation of the PAP. Prolongation of the PAP (with fragmentation seen in the PA 19–20) was correlated with the electrogram to onset of the QRS wave interval that was shown by the red number (ms) above a tracing in the PA 19–20. Red dotted vertical lines denote the onset of QRS waves. The number above a tracing in lead II indicates an interval of successive QRS complexes (that is a cycle length of the VT). A conduction block in the PA (red arrows) resulted in termination of the VT (in the right panel). Abbreviations are given in Fig. 5

isolation of PAP by multiple RF applications immediately below the PA valve. The optimal ablation method for PA-VTs may need to be investigated.

Limitations

There are several limitations to be acknowledged in the present study. First, the number of patients was very small and only one patient had the VA originating above the PA valve. Second, the pacing study from the PA using a 20-polar circumferential catheter was successful only in a patient with the PA-VT, and 1:1 capture loss occurred even at the cycle length of 350 ms and less. This is the major limitation, as the pace and/or activation mapping within the PA is the most important in this study. To characterize the conduction property of PA myocardium, another method using a steerable catheter with appropriate contact force needs to be considered. In addition, it would be necessary to evoke the excitability of PA myocardium in the presence of isoproterenol.

Conclusions

The selective PAP pacing using a 20-polar circumferential catheter was achievable only in a patient with the PA-VT. The slow conduction over the PA myocardium and its junction to RVOT appears to produce the polymorphic changes and alternans of QRS complexes during the PA-VT.

Acknowledgements We thank Drs. Masayuki Sakurai and Akihiko Yotsukura, Hokko Memorial Hospital, and Dr. Minoru Sato, National Hospital Organization Hokkaido Medical Center, for constant encouragement of this study.

Compliance with ethical standards

Conflict of interest We declare that we have no conflict of interest.

References

1. Liao Z, Zhan X, Wu S, Xue Y, Fang X, Liao H, Deng H, Liang Y, Wei W, Liu Y, Ouyang F (2015) Idiopathic ventricular arrhythmias originating from the pulmonary sinus cusp: prevalence, electrocardiographic/electrophysiological characteristics, and catheter ablation. J Am Coll Cardiol 66:2633–2644
2. Liu CF, Cheung JW, Thomas G, Ip JE, Markowitz SM, Lerman BB (2014) Ubiquitous myocardial extensions into the pulmonary artery demonstrated by integrated intracardiac echocardiography and electroanatomic mapping: changing the paradigm of idiopathic right ventricular outflow tract arrhythmias. Circ Arrhythm Electrophysiol 7:691–700
3. Sekiguchi Y, Aonuma K, Takahashi A, Yamauchi Y, Hachiya H, Yokoyama Y, Iesaka Y, Isobe M (2005) Electrocardiographic and electrophysiologic characteristics of ventricular tachycardia originating within the pulmonary artery. J Am Coll Cardiol 45:887–895
4. Tada H, Tadokoro K, Miyaji K, Ito S, Kurosaki K, Kaseno K, Naito S, Nogami A, Oshima S, Taniguchi K (2008) Idiopathic ventricular arrhythmias arising from the pulmonary artery: prevalence, characteristics, and topography of the arrhythmia origin. Heart Rhythm 5:419–426
5. Yamashina Y, Yagi T, Namekawa A, Ishida A, Sato H, Nakagawa T, Sakuramoto M, Sato E, Yambe T (2010) Clinical and electrophysiological difference between idiopathic right ventricular outflow tract arrhythmias and pulmonary artery arrhythmias. J Cardiovasc Electrophysiol 21:163–169
6. Yokoshiki H, Mizukami K, Mitsuyama H, Watanabe M, Tenma T, Tsutsui H (2016) Characteristics of idiopathic ventricular tachycardia originating above the pulmonary valve. Heart Vessels 31:599–607
7. Zhang F, Yang B, Chen H, Ju W, Kojodjojo P, Li M, Gu K, Yang G, Cao K, Chen M (2016) Non-contact mapping-guided ablation of ventricular arrhythmias originating from the pulmonary artery. Europace 18:281–287
8. Zhang J, Tang C, Zhang Y, Su X (2018) Pulmonary sinus cusp mapping and ablation: a new concept and approach for idiopathic right ventricular outflow tract arrhythmias. Heart Rhythm 15:38–45
9. Heeger CH, Kuck KH, Ouyang F (2017) Catheter ablation of pulmonary sinus cusp-derived ventricular arrhythmias by the reversed *U* curve technique. J Cardiovasc Electrophysiol 28:776–777
10. Hsia HH, Scheinman M (2018) Pulmonary sinus of Valsalva arrhythmias: a new twist to an old story. Heart Rhythm 15:46–47
11. Yang Y, Liu Q, Liu Z, Zhou S (2017) Treatment of pulmonary sinus cusp-derived ventricular arrhythmia with reversed *U*-curve catheter ablation. J Cardiovasc Electrophysiol 28:768–775
12. Timmermans C, Rodriguez LM, Crijns HJ, Moorman AF, Wellens HJ (2003) Idiopathic left bundle-branch block-shaped ventricular tachycardia may originate above the pulmonary valve. Circulation 108:1960–1967
13. Lee DI, Park SW, Kook H, Kim W, Kim DH, Lee S, Oh SK, Kim YH (2013) Unusual polymorphic ventricular tachycardia originating from the pulmonary artery. Korean Circ J 43:119–122
14. Nogami A (2015) Mapping and ablating ventricular premature contractions that trigger ventricular fibrillation: trigger elimination and substrate modification. J Cardiovasc Electrophysiol 26:110–115
15. Yagishita A, Yamauchi Y, Sato H, Yamashita S, Hirao T, Usui E, Kawahatsu K, Miyazaki R, Yamaguchi T, Hara N, Umemoto T, Miyamoto T, Obayashi T, Hirao K, Aonuma K (2014) Pulmonary artery isolation for idiopathic polymorphic outflow tract ventricular tachycardia. J Jpn Soc Clin Card Electrophysiol 37:111–118
16. Lerman BB (2015) Mechanism, diagnosis, and treatment of outflow tract tachycardia. Nat Rev Cardiol 12:597–608
17. Hasdemir C, Aktas S, Govsa F, Aktas EO, Kocak A, Bozkaya YT, Demirbas MI, Ulucan C, Ozdogan O, Kayikcioglu M, Can LH, Payzin S (2007) Demonstration of ventricular myocardial extensions into the pulmonary artery and aorta beyond the ventriculo-arterial junction. Pacing Clin Electrophysiol 30:534–539
18. Gami AS, Noheria A, Lachman N, Edwards WD, Friedman PA, Talreja D, Hammill SC, Munger TM, Packer DL, Asirvatham SJ (2011) Anatomical correlates relevant to ablation above the semilunar valves for the cardiac electrophysiologist: a study of 603 hearts. J Interv Card Electrophysiol 30:5–15
19. Yamasaki H, Bertagnolli L, Hindricks G, Arya A (2016) Idiopathic premature ventricular contraction conducting over a ventricle myocardial extension from the pulmonary artery. Pacing Clin Electrophysiol 39:1159–1163

20. Cabo C, Pertsov AM, Baxter WT, Davidenko JM, Gray RA, Jalife J (1994) Wave-front curvature as a cause of slow conduction and block in isolated cardiac muscle. Circ Res 75:1014–1028
21. De la Fuente D, Sasyniuk B, Moe GK (1971) Conduction through a narrow isthmus in isolated canine atrial tissue. A model of the W-P-W syndrome. Circulation 44:803–809
22. Sicouri S, Belardinelli L, Carlsson L, Antzelevitch C (2009) Potent antiarrhythmic effects of chronic amiodarone in canine pulmonary vein sleeve preparations. J Cardiovasc Electrophysiol 20:803–810
23. Postema PG, van Dessel PF, de Bakker JM, Dekker LR, Linnenbank AC, Hoogendijk MG, Coronel R, Tijssen JG, Wilde AA, Tan HL (2008) Slow and discontinuous conduction conspire in Brugada syndrome: a right ventricular mapping and stimulation study. Circ Arrhythm Electrophysiol 1:379–386
24. Cao JM, Qu Z, Kim YH, Wu TJ, Garfinkel A, Weiss JN, Karagueuzian HS, Chen PS (1999) Spatiotemporal heterogeneity in the induction of ventricular fibrillation by rapid pacing: importance of cardiac restitution properties. Circ Res 84:1318–1331
25. Qu Z, Garfinkel A, Chen PS, Weiss JN (2000) Mechanisms of discordant alternans and induction of reentry in simulated cardiac tissue. Circulation 102:1664–1670
26. Watanabe MA, Fenton FH, Evans SJ, Hastings HM, Karma A (2001) Mechanisms for discordant alternans. J Cardiovasc Electrophysiol 12:196–206
27. Sakamoto S, Takagi M, Kakihara J, Hayashi Y, Doi A, Sugioka K, Yoshiyama M (2017) The utility of T-wave alternans during the morning in the summer for the risk stratification of patients with Brugada syndrome. Heart Vessels 32:341–351
28. Sakamoto S, Takagi M, Tatsumi H, Doi A, Sugioka K, Hanatani A, Yoshiyama M (2016) Utility of Tave alternans during night time as a predictor for ventricular fibrillation in patients with Brugada syndrome. Heart Vessels 31:947–956
29. Nakagawa H, Yamanashi WS, Pitha JV, Arruda M, Wang X, Ohtomo K, Beckman KJ, McClelland JH, Lazzara R, Jackman WM (1995) Comparison of in vivo tissue temperature profile and lesion geometry for radiofrequency ablation with a saline-irrigated electrode versus temperature control in a canine thigh muscle preparation. Circulation 91:2264–2273
30. Vaseghi M, Cesario DA, Mahajan A, Wiener I, Boyle NG, Fishbein MC, Horowitz BN, Shivkumar K (2006) Catheter ablation of right ventricular outflow tract tachycardia: value of defining coronary anatomy. J Cardiovasc Electrophysiol 17:632–637
31. Ren JF, Callans DJ, Marchlinski FE (2016) Cautionary pulmonary insufficiency in ablation of ventricular arrhythmias from pulmonary sinus cusps. J Am Coll Cardiol 67:2560–2562